ISSN: 1813-4890

Investigation of the Dynamic Characteristics of Time-Varying Stiffness in Shaft Cracks

Fa Zhou [a], Fuhao Liu [b], Kun Ni [c]

Qingdao University of Technology, Qingdao 266000, China.

[a]fazhou@mvrlab.com, [b]fuhaoliu@mvrlab.com, [c]kunni@mvrlab.com

Abstract

Accounting for the "breathing" phenomenon of shaft cracks, this study derives the moment of inertia of the cracked shaft section based on the dynamic equation of shaft stiffness. Subsequently, a dynamic model of the shaft crack has been established to elucidate the dynamic characteristics of the system influenced by the presence of a shaft crack. This includes an assessment of the variations in the shaft's resistance to bending and torsional rigidities as a function of the rotor's angular position, as well as an analysis of the system's dynamic characteristics consequent to the impact of the shaft crack.

Keywords

Shaft cracks, Dynamic properties, Shaft stiffness.

1. Introduction

At present, the majority of theoretical investigations pertaining to shaft cracks predominantly employ an integrative approach that combines the principles of fracture mechanics with finite element methods[1]. The primary objective is to formulate a model of shaft cracks to analyze the influence of rotor cracks on the dynamic characteristics of the rotor. These explorations have yielded numerous results, laying a solid foundation for the study of the dynamic characteristics of systems affected by shaft cracks[2]. However, most existing studies do not take into account the impact of shaft cracks on gear meshing and the dynamic characteristics of gear systems. In reality, the effect of shaft cracks on gear mesh engagement is substantial and can lead to alterations in the system's dynamic characteristics.

2. Modeling of the axis crack dynamics

Drawing upon the archetype of a helical gear's bend-torsion coupled dynamic model, the variations in shaft stiffness against bending and torsion due to shaft cracking significantly affect the gear meshing model, particularly in the direction of stiffness. Principles of mechanics indicate that a shaft crack will reduce the shaft's resistance to bending and torsion[3]. Additionally, the "breathing" characteristic of the shaft crack leads to a time-varying nature in the shaft's stiffness against bending and torsion as the shaft continues to rotate[4-5].

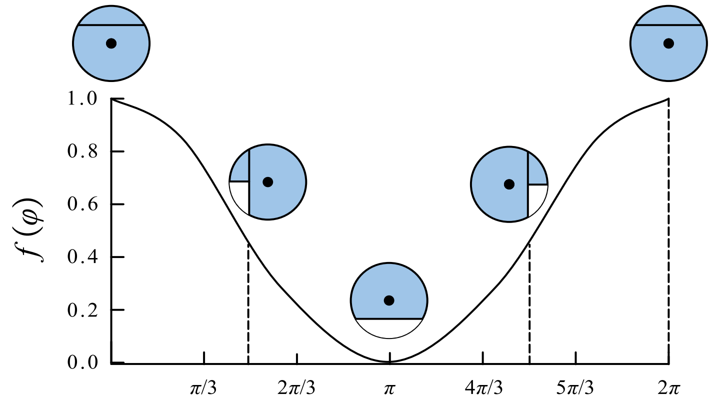

Fig.1 The process of shaft crack opening and closing

When the crack is closed, the stiffness of the shaft crack element can be approximated as equivalent to that of a normal shaft element. However, when the crack is fully open, the reduction in stiffness of the shaft crack element is at its maximum. During the operation of the equipment, the shaft crack is predominantly in a transitional state. Throughout this period, the reduction in stiffness varies over time. Considering the characteristic time-varying stiffness of the shaft crack element, a cosine wave model is employed to simulate the opening and closing patterns of shaft cracks. The cosine wave model accounts for the transitional process where the shaft crack is partially open and partially closed. The patterns of opening and closing are illustrated. The time-varying stiffness of the axis in the direction of the shaft crack can be represented by a computation expression as follows:

$$K_{xt} = K_h - f\left(t\right)\Delta K_x \tag{1}$$

$$\Delta K_x = K_{xc} - K_{xo} \tag{2}$$

Where $\triangle K_x$is the change of the bending stiffness of the shaft to the x axis; K_h is the bending stiffness of the healthy axis segment; K_{xc} is the bending stiffness of the x axis when the axis crack is fully closed, that is, the bending stiffness of the shaft to the x axis in health condition; K_{xo} is the bending stiffness of the x axis when the axis crack is fully open. The calculated expression for the time-varying bending stiffness K_{yt} in the axis crack y-axis direction can be expressed as:

$$K_{yt} = K_h - f\left(t\right)\Delta K_y \tag{3}$$

$$\Delta K_y = K_{yc} - K_{yo} \tag{4}$$

Among them, $\triangle K_y$ is the change of the bending stiffness of the shaft for the y axis; K_{yc} is the bending stiffness of the shaft for the y axis, which is equal to the bending stiffness of the shaft for the y axis in healthy state; $K_{yo}$is the bending stiffness of the shaft crack for the y axis; based on the "breathing" characteristic of the bending stiffness when the shaft crack is completely closed:

$$K_{xc} = K_h \tag{5}$$

$$K_{yc} = K_h \tag{6}$$

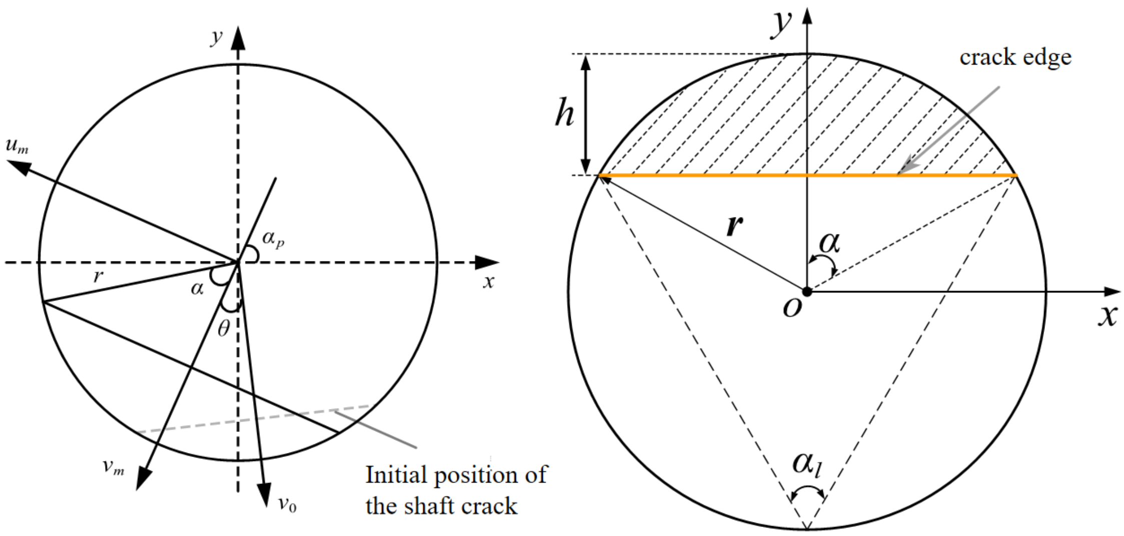

Fig.2 Axis crack cross-section model

The fixed coordinate system xoy of the axis and the open and closed coordinate system $u_m o v_m$ of the axis crack exist. Where α is the circumference of the crack; r is the radius of the axis; α_p is 70°; α_l is the circumference of the crack; h is the crack depth. Undimensional crack depth λ is expressed as:

$$\lambda = \frac{h}{2r_s} \tag{7}$$

α can be expressed as:

$$\alpha = \arccos\left((r-h)/r\right) \tag{8}$$

Since it is difficult to obtain K_{xo} and K_{yo} directly, thus can be calculated by calculating the shaft crack when fully open, Curending stiffness u_m of the axis for K_{umo} axis and bending stiffness v_m of the axis for K_{vmo} axis, The results are then obtained by transforming the relationship between the coordinate systems.among:

$$K_h = \frac{12EI}{l^3} \tag{9}$$

$$I = \frac{\pi d^4}{64} \tag{10}$$

The torsional stiffness can be expressed as:

$$K_p = \frac{GI_p}{l} \tag{11}$$

Where I_p is the polar moment of inertia of the axis, which can be expressed as:

$$I_p = \frac{\pi d^4}{32} \tag{12}$$

As the crack expands, the moment of inertia of the crack also changes. The moment of inertia for the axis v_m axis is:

$$
\begin{aligned}
I_{vmo1} &= \int_A u_m^2 dA = \iint_D \left(r\sin\theta \right)^2 r dr d\theta \\
&= \int_{\alpha}^{2\pi-\alpha} \sin^2\theta d\theta \int_0^{\frac{d}{2}} r^3 dr \\
&= \int_{\alpha}^{2\pi-\alpha} \frac{1-\cos 2\theta}{2} d\theta \int_0^{\frac{d}{2}} r^3 dr \\
&= \frac{1}{2}\left[\theta - \frac{1}{2}\sin 2\theta \right]_{\alpha}^{2\pi-\alpha} \cdot \left[\frac{r^4}{4} \right]_0^{\frac{d}{2}} \\
&= \frac{\pi d^4}{64}\left(1 - \frac{\alpha}{\pi} + \frac{\sin 2\alpha}{2\pi} \right)
\end{aligned}
\tag{13}
$$

$$
\begin{aligned}
I_{vmo2} &= \int_A u_m^2 dA = \frac{1}{2}\iint_D u_m^2 du_m dv_m \\
&= \frac{1}{2}\int_{-r\sin\alpha}^{r\sin\alpha} u_m^2 du_m dv_m \\
&= \frac{1}{2}\left[u_m^3 \right]_{-r\sin\alpha}^{r\sin\alpha} \cdot \frac{1}{3}\left[v_m \right]_0^{r\cos\alpha} \\
&= \frac{\pi d^4}{64}\left(\frac{\sin 2\alpha}{3\pi} - \frac{\sin 4\alpha}{6\pi} \right)
\end{aligned}
\tag{14}
$$

$$
I_{vmo} = I_{vmo1} + I_{vmo2} = \frac{\pi d^4}{64}\left(1 - \frac{\alpha}{\pi} + \frac{5\sin 2\alpha}{6\pi} - \frac{\sin 4\alpha}{6\pi} \right) \tag{15}
$$

Therefore, when the crack is fully opened, the bending stiffness of the shaft for the u_m shaft is:

$$
K_{umo} = \frac{I_{vmo}}{I} K_h \tag{16}
$$

The moment of inertia for axis u_m is:

$$
\begin{aligned}
I_{umo1} &= \int_A v_m^2 dA = \iint_D \left(r\cos\theta \right)^2 r dr d\theta \\
&= \int_{\alpha}^{2\pi-\alpha} \cos^2\theta d\theta \int_0^{\frac{d}{2}} r^3 dr \\
&= \int_{\alpha}^{2\pi-\alpha} \frac{\cos 2\theta + 1}{2} d\theta \int_0^{\frac{d}{2}} r^3 dr \\
&= \frac{1}{2}\left[\frac{1}{2}\sin 2\theta + \theta \right]_{\alpha}^{2\pi-\alpha} \cdot \left[\frac{r^4}{4} \right]_0^{\frac{d}{2}} \\
&= \frac{\pi d^4}{64}\left(1 - \frac{\alpha}{\pi} - \frac{\sin 2\alpha}{2\pi} \right)
\end{aligned}
\tag{17}
$$

$$\begin{aligned} I_{umo2} &= \int_A v_m^2 dA = \frac{1}{2}\iint_D v_m^2 du_m dv_m \\ &= \frac{1}{2}\int_{-r\sin\alpha}^{r\sin\alpha} du_m \int_0^{r\cos\alpha} v_m^2 dv_m \\ &= \frac{1}{2}\left[u_m\right]_{-r\sin\alpha}^{r\sin\alpha} \square \frac{1}{3}\left[v_m^3\right]_0^{r\cos\alpha} \\ &= \frac{\pi d^4}{64}\left(\frac{\sin 2\alpha}{3\pi} + \frac{\sin 4\alpha}{6\pi}\right) \end{aligned} \tag{18}$$

$$I_{umo} = I_{umo1} + I_{umo2} = \frac{\pi d^4}{64}\left(1 - \frac{\alpha}{\pi} - \frac{\sin 2\alpha}{6\pi} + \frac{\sin 4\alpha}{6\pi}\right) \tag{19}$$

Therefore, when the crack is fully opened, the bending stiffness of the shaft for the u_m shaft is:

$$K_{vmo} = \frac{I_{umo}}{I} K_h \tag{20}$$

According to the coordinate system relationship, after the coordinate transformation, the bending stiffness of the axis for the x -axis is:

$$K_{xo} = \sqrt{K_{vmo}^2 \cos^2\alpha_p + K_{umo}^2 \sin^2\alpha_p} \tag{21}$$

According to the coordinate system relationship, after the coordinate transformation, the bending stiffness of the axis for the y-axis is:

$$K_{yo} = \sqrt{K_{vmo}^2 \sin^2\alpha_p + K_{umo}^2 \cos^2\alpha_p} \tag{22}$$

The torsion resistance stiffness is:

$$K_p' = \frac{GI_p'}{l} \tag{23}$$

Where the I'_p is:

$$I_p' = I_{vmo} + I_{umo} \tag{24}$$

Therefore, the variation of the torsional stiffness is:

$$\Delta K_z = K_p - K_p' \tag{25}$$

Therefore, the torsion stiffness matrix of axial bending under the influence of shaft crack can be expressed as:

$$K' = \begin{pmatrix} K_h - f(t)\Delta K_x & 0 & 0 \\ 0 & K_h - f(t)\Delta K_y & 0 \\ 0 & 0 & K_p - f(t)\Delta K_z \end{pmatrix} \tag{26}$$

3. The influence of shaft crack on the bending and coupling stiffness of the system

In this section, the driving wheel rotates clockwise with an input speed and torque of 5000 rpm and 50 N·m, respectively, with the initial phase of the shaft crack set at 0. Given the time-varying nature of the shaft crack, the depth of the crack or, equivalently, the size of the circumferential angle has a significant impact on stiffness. Investigating the stiffness against bending and torsion within the dynamic model of a geared shaft system with varying crack depths allows for characterizing the influence of different crack depths on stiffness. The time-varying curves of stiffness in the direction of the crack shaft section with different crack depths are depicted in Figure 3 and Figure4.

Upon the emergence of a shaft crack, the bending stiffness in both (x) and (y) directions of the crack shaft section exhibits periodic variation, with the rotation cycle of the driving wheel aligning with the cycle of stiffness variation. This observation is in line with the "breathing" characteristic attributed to shaft cracks. Under healthy conditions, the bending stiffness in both (x) and (y) directions of a shaft element is 27820.7 kN/mm. At a non-dimensional crack depth of 0.5, the minimum bending stiffness in the crack shaft element direction is 25240.5 kN/mm, while in the (y) direction, the minimum value is 17498.5 kN/mm. When the non-dimensional crack depth reaches 1, the minimum bending stiffness values in both the (x) and (y) directions fall to 13910.6 kN/mm, nearly half of the stiffness of a healthy shaft section, corroborating with related research , thus confirming the model's accuracy. At a crack depth of 1.5, the minimum values are 4349.8 kN/mm in the (x) direction and 11130.1 kN/mm in the (y) direction.

The magnitude of the periodic changes in bending stiffness varies with time and is not uniform across different crack depths or directions. At a non-dimensional crack depth of 0.5, the bending stiffness in the (x) direction varies periodically within the range of 25240.5 kN/mm to 27820.7 kN/mm, while in the (y) direction, it oscillates between 17498.5 kN/mm and 27820.7 kN/mm. At a non-dimensional crack depth of 1, both the (x) and (y) direction stiffness values vary periodically within the range of 13910.6 kN/mm to 27820.7 kN/mm. Comparing the variation magnitude for non-dimensional crack depths of 0.5 and 1 in the (x) direction reveals that greater crack depths result in larger periodic changes in both (x) and (y) direction bending stiffness. Furthermore, comparing the stiffness variations for a crack depth of 0.5 indicates that the impact on the (x) direction surpasses that on the (y) direction, illustrating an asymmetric influence on stiffness, with the (x) directional stiffness exhibiting a greater reduction than in the (y) direction.

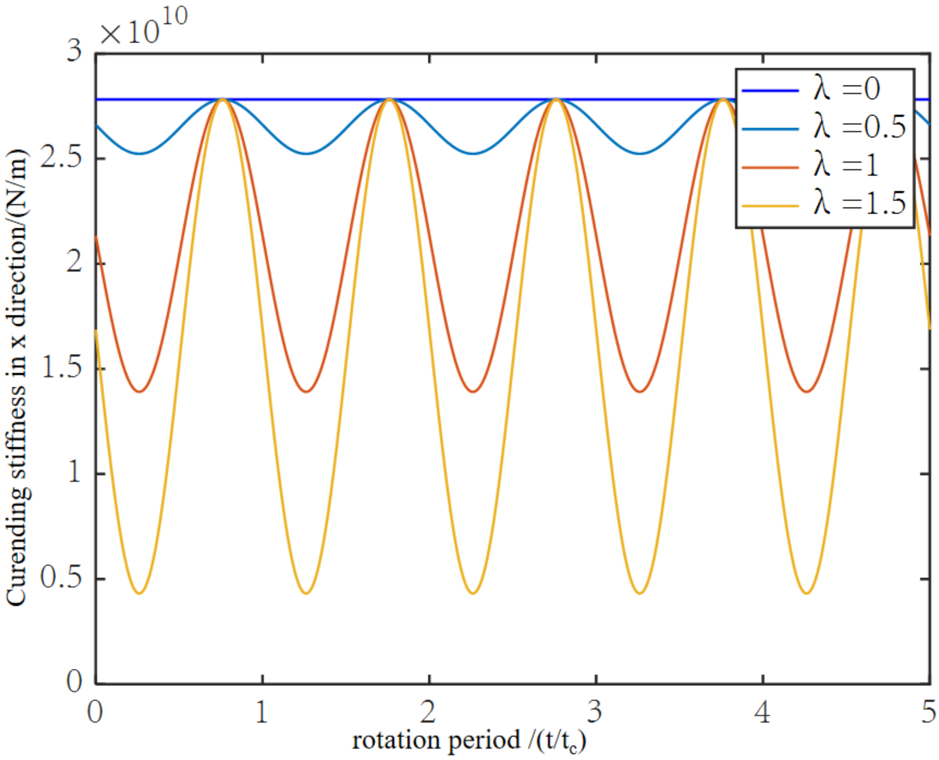

Fig.3 Curending stiffness in x direction under different crack depth in the crack shaft section

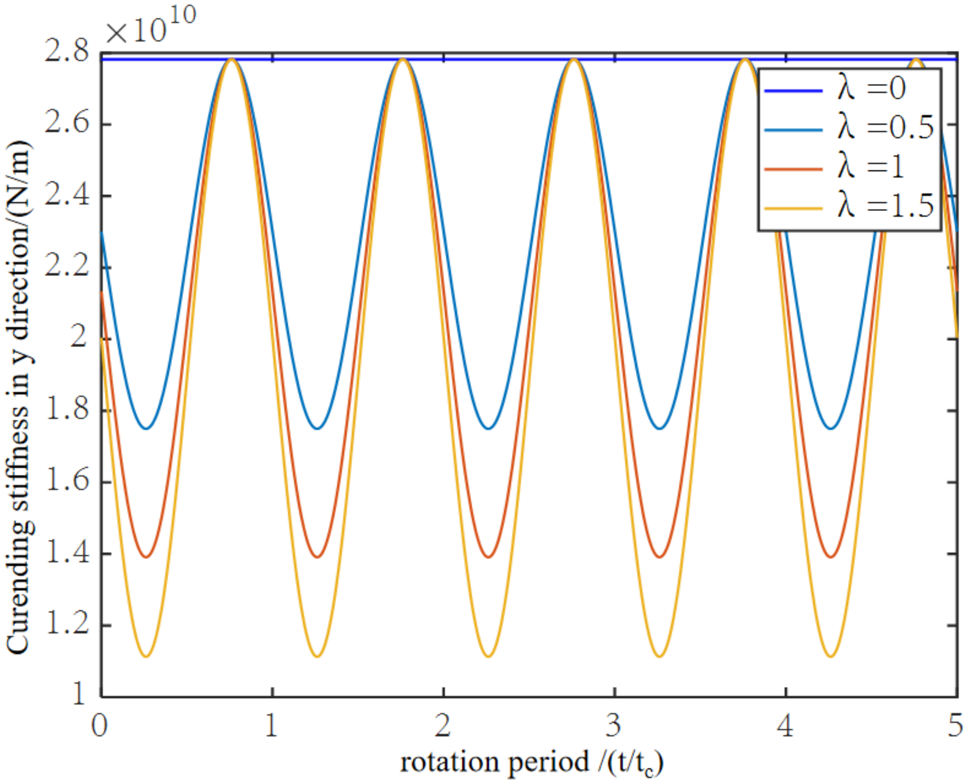

Fig.4 Curending stiffness in dy direction at different crack depths of crack shaft segments

4. Conclusion

A comparative analysis of the bending stiffness in both (x) and (y) directions, as well as the torsional stiffness of the shaft section with varying crack depths, has been conducted. It has been observed that the stiffness of the crack-affected shaft section reduces with the increase in the depth of the crack. Notably, when the crack depth reaches half the diameter of the rotor, the stiffness is also reduced to half of its normal value. This empirical validation substantiates the accuracy of crack theory and lays the groundwork for subsequent analyses of the effects of shaft cracking on the integrity of the system.

References

[1] H.T. Ping : *Dynamic Coupling Modeling of Shaft Crack and Gear Faults and Simulation Analysis*(MS. Chongqing University,China 2018). p.93

[2] Y.B. Zhao, *Fault characteristics and location quantitative identification of cracked hollow shaft rotor of heavy duty gas turbine*[C]. (Construction Machinery). Vol.54 (2023) No.5,p. 43-53

[3] Y. Shen, X.G. Zhang and H. Jing: *Comparative Study on Dynamic Characteristics of Two-stage Gear System with Gear and Shaft Cracks Considering the Shaft Flexibility*[J]. in IEEE Access, vol. 8, pp. 133681-133699, 2020, doi: 10.1109/ACCESS.2020.3009398.

[4] Francis, Anjana, and C, Muruganantham: *An Adaptive Denoising Method using Empirical Wavelet Transform*. (International Journal of Computer Applications) 117. 21(2015):18-20.

[5] M. Chouksey, and A. Parey: *Measurement of FRFs of coupled geared rotor system and the development of an accurate finite element model*. (Mechanism & Machine Theory) 123(2018):66- 75.